

1 **Amine Volatilization from Herbicide Salts: Implications for Herbicide Formulations**
2 **and Atmospheric Chemistry**

3
4 **Stephen M. Sharkey,^a Anna M. Hartig,^a Audrey J. Dang,^a Anamika Chatterjee,^a Brent**
5 **J. Williams,^a and Kimberly M. Parker^{*a}**

6 ^aDepartment of Energy, Environmental, and Chemical Engineering, Washington University
7 in St. Louis, St. Louis, Missouri 63130, United States

8 *Corresponding author: kmparker@wustl.edu, phone: (314) 935-3461; fax: (314) 935-7211.

9
10 Word count: 4,587

11 4 Figures (word-equivalents: 1,800)

12 Total word-equivalents: 6,387
13
14

15 **Abstract**

16 Amines are frequently included in formulations of the herbicides glyphosate, 2,4-D, and
17 dicamba to increase herbicide solubility and reduce herbicide volatilization by producing
18 herbicide-amine salts. Amines, which typically have higher vapor pressures than the
19 corresponding herbicides, could potentially volatilize from these salts and enter the
20 atmosphere, where they may impact atmospheric chemistry, human health, and climate. Amine
21 volatilization from herbicide-amine salts may additionally contribute to volatilization of
22 dicamba and 2,4-D. In this study, we established that amines applied in herbicide-amine salt
23 formulations undergo extensive volatilization. Both dimethylamine (DMA) and
24 isopropylamine (IPA) volatilized when aqueous salt solutions were dried to a residue at ~20°C,
25 while lower vapor pressure amines like diglycolamine (DGA) and n,n-bis-(3-
26 aminopropyl)methylamine (BAPMA) did not. However, all four amines volatilized from salt
27 residues at 40-80°C. Because amine loss typically exceeded herbicide loss, we proposed that
28 neutral amines dominated volatilization, and that higher temperatures altered their protonation
29 state and vapor pressure. Due to an estimated 4.0 Gg N/yr applied as amines to major U.S.
30 crops, amine emissions from herbicide-amine salts may be important on regional scales.
31 Further characterization of worldwide herbicide-amine use would enable this contribution to
32 be compared to the 285 Gg N/yr of methylamines emitted globally.

33 **Synopsis**

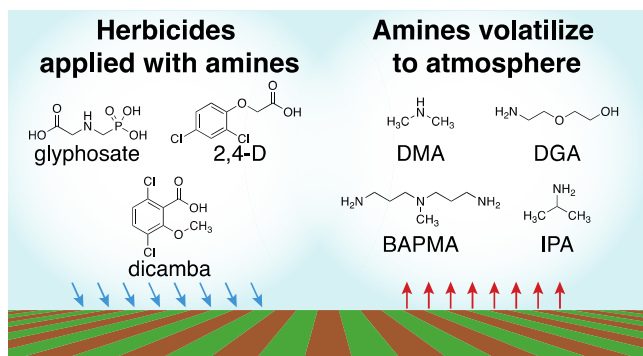
34 Amines applied in herbicide-amine salt formulations volatilize to the atmosphere, potentially
35 contributing to herbicide volatilization. In the atmosphere, these amines are expected to affect
36 atmospheric chemistry with implications for human health and climate.

37

38 **Key words:** glyphosate, dicamba, 2,4-dichlorophenoxyacetic acid (2,4-D), agrochemicals,
39 alkylamines

40

41 **TOC Art**



42

43 **Introduction**

44 Herbicides are widely used in agriculture globally. In the U.S. alone, an estimated 260
45 Gg of herbicides were applied in 2019.¹ In addition to the herbicide itself, herbicide
46 formulations typically contain supplemental chemicals to modify the herbicide's properties.²
47 For example, glyphosate, the most used herbicide in the U.S.,³ is often formulated with an
48 amine counterion. In 2017, 55% of glyphosate applied to soybeans, cotton, and wheat was
49 applied with an amine (i.e., isopropylamine (IPA), dimethylamine (DMA)).⁴ These amines are
50 included in formulations at an equimolar concentration to increase the solubility of glyphosate,
51 as well as other herbicides (i.e., 2,4-dichlorophenoxyacetic acid (2,4-D)), by deprotonating the
52 acidic herbicide to form a salt.^{5,6}

53 Beyond solubility, semi-volatile herbicides like 2,4-D and dicamba (3,6-dichloro-2-
54 methoxybenzoic acid) are formulated as amine salts to reduce their vapor pressure and thereby
55 prevent off-target damage to other vegetation resulting from herbicide drift.⁷⁻⁹ Concerns about
56 the drift of these two herbicides have been amplified since the release of genetically modified
57 (GM) crops that tolerate 2,4-D and dicamba in 2014-2015.² Although the postemergent use of
58 2,4-D and dicamba on GM tolerant crops has been considered imperative to overcome the
59 reduced effectiveness of glyphosate,^{10,11} this practice has been jeopardized by widespread
60 damage to non-tolerant crops associated with their drift.² Drift of these herbicides may also
61 impact yields of other fruits and vegetables,¹²⁻¹⁵ function of neighboring ecosystems,¹⁶ and the
62 emergence of resistant weeds.¹⁷ While additional processes including spray drift can contribute
63 to off-target herbicide movement,¹⁸ herbicide volatilization, which can occur for days after
64 application,^{19,20} contributes significantly to drift even when amine-salt formulations are
65 used.^{2,21} To prevent volatilization, dicamba applications on GM tolerant crops are restricted to
66 formulations that include diglycolamine (DGA) or n,n-bis-(3-aminopropyl)methylamine
67 (BAPMA), which have reduced herbicide volatilization^{19,20,22-27} relative to older DMA

68 formulations.^{28,22,19,23,24} Unfortunately, herbicide volatilization from GM tolerant crops has
69 remained a persistent challenge despite these advances.²

70 Notably, the volatilization of amines themselves has not been investigated, even though
71 the amines included in formulations have higher vapor pressures than the herbicides (**SI Table**
72 **S1**). The loss of amines to the atmosphere may promote herbicide volatilization leading to
73 heightened off-target drift damage. In addition, volatilized amines may affect atmospheric
74 processes that impact health and climate. Despite their widespread use, herbicide-amine salt
75 formulations have not been considered alongside other anthropogenic sources of amine
76 pollution to the atmosphere (e.g., animal husbandry, industry).²⁹ Amine vapors oxidize to form
77 potential carcinogens such as nitrosamines and nitramines.³⁰⁻³⁵ Both the parent amines and
78 their oxidation products contribute to formation and growth of particles in the atmosphere,³⁶⁻
79 ³⁸ which influences the climate³⁹⁻⁴¹ and negatively impacts human health.⁴² For example,
80 polystyrene particles modified to have amine functional groups present on their surface have
81 been associated with greater deleterious health outcomes in laboratory animals compared to
82 unmodified polystyrene particles.^{43,44}

83 In this study, we experimentally evaluated amine loss from herbicide-amine salt
84 formulations, as well as confirmed that amine vapor was detectable above herbicide-amine
85 solutions. By measuring co-occurring losses of amine and dicamba, we proposed underlying
86 processes that may contribute to volatilization of both components. Integrating available data,
87 we estimated the magnitude of amine input into the environment from herbicide-amine salts
88 relative to other known sources of amine pollution.

89 **Materials and Methods**

90 *Experimental Approach*

91 Chemicals, suppliers, and glassware cleaning procedures can be found in the
92 Supporting Information (**SI Section S1**). Due to inhalation hazards, open vessels with amines

93 were handled in a fume hood. Stock solutions of all chemical components were prepared in
94 Milli-Q water, with the exception of 2,4-D free acid that was prepared in ~40/60 (v/v)
95 acetonitrile/water due to low aqueous solubility.⁴⁵

96 ***Measurement of Amine and Herbicide Losses from Salts***

97 Expanding on prior protocols,²⁴ herbicide-amine residues were dried from a 2.0 mL
98 aqueous solution of amine and herbicide at an equimolar concentration of 123 μM in a 50 mL
99 glass beaker (VWR catalog number 13912–149), resulting in an expected amount of 246
100 nmoles of dicamba and amine each present (n_x^{expected} , where x corresponds to the constituent
101 measured). When the number of moles in solution were measured (n_x^{soln}), 2.3 mL of solution
102 was prepared instead of 2.0 mL so that the additional 300 μL aliquot could be taken for
103 derivatization and quantification of the amine. The solutions were dried in a fume hood at room
104 temperature ($\sim 22^\circ\text{C}$) for 24 h before at least two beakers were extracted to determine the moles
105 remaining in the herbicide-amine residue after drying ($n_x^{0\text{ h,dried}}$). To determine moles lost
106 during drying, we calculated the difference between the molar quantity expected initially in
107 solution and the measured value in the dried residue after 24 h ($n_x^{\text{expected}} - n_x^{0\text{ h,dried}}$). We chose
108 24 h because it allowed for evaporation of all visible water from the beaker. To measure
109 volatilization from residues at high temperatures, the remaining beakers containing the dried
110 residues (prepared in triplicate) were then placed on hot plates at elevated temperatures for a
111 time (t) before extraction to determine moles remaining ($n_x^{t,\text{dried}}$). To compare losses from the
112 residue phase, we elevated the temperature to 40°C for 48 h before measuring remaining molar
113 quantity to calculate the difference in moles remaining ($n_x^{0\text{ h,dried}} - n_x^{48\text{ h,dried}}$). We chose 48 h
114 for most experiments because it allowed for enough volatilization for comparison between the
115 different herbicide-amine salts. To control for any environmental conditions (e.g., relative
116 humidity) that may influence results, all data included in individual figure panels were
117 collected from experiments conducted simultaneously.

118 ***Analysis of Solution and Residue Composition***

119 Residues were extracted with 2 mL of a 50/50 (v/v) acetonitrile/water mixture (**SI**
120 **Section S2**). To improve subsequent analysis, samples containing glyphosate were instead
121 extracted with 2 mL of 100% water (**SI Section S3**). Each extract was divided into 1 mL for
122 direct quantification of dicamba or 2,4-D (when applicable) and 300 μ L for amine and/or
123 glyphosate derivatization. Extracted aliquots were stored at 4°C in 2 mL vials until
124 derivatization or quantification. Amines and glyphosate were derivatized using 9-
125 fluorenylmethyloxycarbonyl chloride (FMOC-Cl) based on a prior method⁴⁶ (**SI Sections S4,**
126 **S5**). Dicamba, 2,4-D, derivatized amines, and derivatized glyphosate were quantified on
127 HPLC-UV (**SI Section S6**).

128 ***Gas Phase Amine Detection***

129 IPA was measured in the headspace of 20 mL amber glass vials (Thermo Scientific
130 catalog number B7921VO) containing 100 μ L solutions by *in situ* TD GC-MS (**SI Section S7**).
131 Measurements were performed on four sets of six glyphosate-IPA solutions and three sets of
132 five glyphosate-only solutions, with each included constituent diluted in water to 13.2 mM.
133 Vials were sampled individually; one gas phase measurement was taken immediately after
134 sample set preparation and every 20 min thereafter. The IPA GC peak was positively identified
135 with a calibration standard as well as comparison with a library mass spectrum⁴⁷ (**SI Figure**
136 **S6**).

137 **Results and Discussion**

138 ***Amine Losses from Herbicide-Amine Salts During Formulation Drying***

139 Herbicide-amine salts are applied as aqueous solutions that subsequently dry to produce
140 residues on leaf or soil surfaces.² We first measured changes in the remaining amounts of DMA
141 and 2,4-D when solutions prepared with equimolar concentrations of the two constituents were
142 dried to generate residues at room temperature over 24 h (**Figure 1A**). While the amount of

143 2,4-D was unchanged, the remaining moles of DMA decreased by $25\pm 2\%$. The majority of this
144 loss occurred between 12 and 16 h, which corresponded to complete evaporation of visible
145 water. Consequently, the transition from aqueous solution to dried residue appears to drive
146 DMA volatilization at ambient temperatures possibly due to the change in protonation state of
147 the amine as the aqueous solution dries to a residue.

148 We expanded our investigation to compare the losses of DMA and IPA from salts
149 prepared with three different herbicides (i.e., dicamba, glyphosate, 2,4-D) corresponding to
150 combinations used in practice⁴ (**Figure 1B**). For all six DMA and IPA salts, we observed that
151 amine losses, which ranged from 90 ± 22 to 219 ± 11 nmoles over the experiment duration
152 (**Figure 1B**), greatly exceeded losses of the corresponding herbicides ($n_{herbicide}^{expected} -$
153 $n_{herbicide}^{48 h, dried} < 23$ nmoles, **SI Figure S7**). Losses of amines from all salts occurred during both the
154 drying period ($n_x^{expected} - n_x^{0 h, dried}$) and from the residue phase at elevated temperature
155 ($n_x^{0 h, dried} - n_x^{48 h, dried}$). DMA was consistently lost to a greater extent than IPA, likely
156 corresponding to ~3-fold higher vapor pressure of DMA relative to IPA (**SI Table S1**). While
157 amine losses tended to be moderately higher from glyphosate salts than dicamba and 2,4-D
158 salts, amine losses were significant from all combinations regardless of herbicide type
159 indicating that similar phenomena may drive volatilization in all cases.

160 Using *in situ* thermal desorption gas chromatography–mass spectrometry (TD GC-MS),
161 we confirmed that amine volatilization contributed to amine loss by measuring the presence of
162 IPA in the headspace above glyphosate-IPA salt solutions concentrated ~100-fold to reflect
163 conditions during drying (**Figure 1C**). Though IPA was consistently detected in the headspace
164 (confirmed by library comparison),⁴⁷ we observed a highly variable amount of IPA. Additional
165 analysis at 6 time points spanning a 100 min period indicated that the amine flux from these
166 concentrated solutions was highly dynamic (**SI Section S9**), likely contributing to variability
167 in the measured amounts of IPA among samples because our method only permitted sampling

168 for 5 min for each 20 min cycle rather than continuous measurement. Additional variability
169 may also result from minor differences in sensitivities between instrument collection channels
170 (SI Section S9). To exclude interference due to thermal decomposition of glyphosate into
171 amine products,^{48,49} we also analyzed solutions prepared without IPA (Figure 1C). We
172 observed that no IPA was detected with the exception of the first control sample analyzed
173 (Rep.1), which we attributed to minor carryover of IPA from analysis of the IPA-containing
174 samples (SI Section S9). Consequently, volatilized IPA from the glyphosate-IPA salt solution
175 was the dominant contribution to the IPA measured in the headspace of the IPA-containing
176 samples (Figure 1C).

177 *Amine and Dicamba Losses from Dicamba-Amine Salts*

178 After demonstrating that amines volatilize from all herbicide-amine salts tested (Figure
179 1B), we next aimed to elucidate key factors that may control amine volatilization from
180 herbicide-amine salts (e.g., vapor pressure, amine-dicamba interactions). We investigated these
181 factors by testing experimental variables including temperature, experiment duration, and the
182 initial ratio of amine to herbicide in solution. In these experiments, we monitored the loss of
183 the herbicide dicamba alongside amines, which also tested the effect of amine loss on dicamba
184 volatilization.

185 One important parameter is temperature, which we hypothesized would increase the
186 vapor pressure of the molecules, as well as alter additional factors (e.g., protonation state)⁵⁰⁻⁵⁴
187 particularly in the dried residue phase. Elevated temperature consistently increased the loss of
188 both DMA (Figure 2A) and IPA (Figure 2B) from residues over 48 h. Consistent with previous
189 work,²⁴ dicamba losses were significant at higher temperatures (i.e., 60°C or 80°C). However,
190 the lower loss of dicamba relative to the amines, particularly at moderate temperatures (i.e.,
191 40°C or 60°C), suggests that at least some of the amines are lost from the residue as neutral

192 molecules rather than dicamba-amine ion pairs and that the extents of proton transfer from
193 dicamba to the amines are possibly incomplete in our residues.

194 We expanded the amines studied to include DGA (**Figure 2C**) and BAPMA (**Figure**
195 **2D**), which are used in specific formulations intended to prevent dicamba volatilization.¹⁸
196 Unlike DMA and IPA, neither DGA nor BAPMA were lost to measurable extents during drying
197 (**SI Section S2**), possibly due to their lower vapor pressures compared to DMA and IPA (**SI**
198 **Table S1**). DGA's low pure phase vapor pressure is likely due to the intermolecular hydrogen
199 bonds between alcohol and amine groups that are present in ethanolamines,⁵⁵ which increase
200 the enthalpy of vaporization.⁵⁶ We expect that the additional hydrogen bonding groups present
201 on DGA compared to DMA and IPA have a similar impact in our residues, which limits the
202 volatilization of DGA. Like DMA and IPA, DGA loss increased consistently with increasing
203 temperature; however, dicamba loss was only measurable at the highest temperature (i.e.,
204 80°C). Surprisingly, among the four amines, BAPMA loss was highest at the lower
205 temperatures (20°C and 40°C) but did not increase further at higher temperatures (**Figure 2D**).
206 Dicamba loss from the dicamba-BAPMA salt residue was also uniquely absent at all
207 temperatures possibly due to the two additional amine functional groups present on BAPMA.

208 At selected temperatures, we extended the experiment duration to determine if amine
209 loss resulted in greater dicamba loss over longer times (**Figure 3A-C**). We observed that DMA
210 loss during drying was two-fold higher than in other experiments in this study (e.g., **Figure**
211 **1B**), which we attributed to seasonal variations in laboratory ambient conditions (e.g., relative
212 humidity) that were controlled by exclusively comparing data collected simultaneously. We
213 observed that DMA loss from the final residue at both 40°C and 60°C continued until at least
214 96 h, resulting in ~80% loss at 40°C (**Figure 3A**) and near-complete loss at 60°C (**Figure 3B**).
215 Despite extensive DMA loss at both temperatures, dicamba loss was much greater at 60°C,
216 approaching near-completion though lagging DMA loss. In contrast, dicamba loss at 60°C was

217 lower in the presence of DGA, which also exhibited reduced loss relative to DMA at the same
218 temperature (**Figure 3C**). Consequently, dicamba loss from the residue phase at longer times
219 was influenced by the temperature, but also the identity and remaining amount of the amine.

220 To gain further insight into the influence of amine amount on dicamba loss, we
221 investigated how the molar ratio of amine to dicamba affects the loss of each component during
222 and after drying. To examine co-occurring losses of amine (i.e., DMA) and dicamba during
223 drying, we reduced the amount of DMA in the initial solution while holding dicamba
224 concentration constant (**Figure 3D**). At lower DMA/dicamba ratios, we observed, for the first
225 time in this study, dicamba loss during drying at room temperature. In contrast, DMA loss
226 during drying decreased at lower ratios and was not measurable loss from solutions prepared
227 with $0.25/1 \ n_{DMA}^{expected} / n_{dicamba}^{expected}$ (**Figure 3D**). We hypothesize that the reduced DMA loss
228 measured at lower ratios is due to the remaining fraction of DMA being ionic, and therefore
229 less volatile, after undergoing proton transfer with dicamba.

230 To examine amine and dicamba losses from the dried residue, we selected DGA, which
231 is not lost during drying, so that the initial ratio of DGA/dicamba in the dried residue could be
232 controlled. Reducing the ratio of $n_{DMA}^{expected} / n_{dicamba}^{expected}$ in the initial solution from 1/1 to 0.75/1
233 led to less DGA loss when subjected to elevated temperature (60 °C) after drying (**Figure 3E**).
234 However, unlike DMA loss during drying, DGA loss after drying remained measurable even
235 at lower DGA/dicamba ratios (**Figure 3E**). Consistent with prior results conducted at 40°C,²⁴
236 dicamba loss at 60°C increased at lower DGA/dicamba ratios (**Figure 3E**). Under conditions
237 where the starting amount of DGA was reduced, dicamba volatilization exceeded that of DGA,
238 indicating that dicamba may also be lost as a neutral molecule from our residues. Unlike with
239 the reduced DMA/dicamba residues from which DMA loss was no longer measurable at 0.25/1
240 $n_{DMA}^{expected} / n_{dicamba}^{expected}$ ratio, we did not reach a ratio where DGA loss was no longer measurable.
241 This could be due to the changing amount of dicamba present in the residues as it volatilized,

242 as well as the higher temperature (i.e., 60°C versus 20°C used in the DMA experiments) both
243 increasing the volatility of DGA and decreasing the extent of proton transfer to form additional
244 volatile neutral DGA molecules.

245 *Possible Factors Influencing Dicamba and Amine Volatilization*

246 In the initial dilute aqueous solutions, we expect that deprotonation of the acidic
247 herbicides (pK_a 1.9-2.7, **SI Table S1**) and protonation of the basic amines (pK_a 9.6-10.7, **SI**
248 **Table S1**) occur via water-mediated proton transfer, resulting in a pair of non-volatile ions.
249 The ionic speciation, coupled with other possible factors (e.g., rates of air-water exchange of
250 the neutral molecules), prevents volatilization of both the amine and the herbicide (**Figure 1A,**
251 **0-12 h**). As water evaporates, the solutes change from minor components in the aqueous
252 solution to major components in the dried residue. Although additional characterization of the
253 dried herbicide-amine residue is needed, we anticipate that, depending on the melting point, it
254 may behave analogously to a protic ionic liquid (PIL) or a solid (cocrystal/salt). Both dicamba-
255 DGA and dicamba-BAPMA have been found to be liquids at room temperature,⁵⁷ but to our
256 knowledge the phases of the other dicamba-amine residues included in this study have not been
257 reported. However, it should be noted that the characterization of PILs (including dicamba-
258 DGA and dicamba-BAPMA)⁵⁷ has been typically carried out in the absence of water, whereas
259 some water likely remains in our herbicide-amine residues⁵⁸ (as well as likely dried herbicide-
260 amine residues in the field) and may affect molecular speciation and volatilization by altering
261 intermolecular interactions.^{59,60}

262 Molecules in PILs will be distributed between their neutral and ionic species according
263 to the extent of proton transfer (i.e., HA + B ↔ A⁻ + HB⁺).^{50,61,62} Although the extent of proton
264 transfer in PILs correlates with the difference in the aqueous-phase pK_a values of the acid and
265 base (ΔpK_a),^{50,62,63} deviations from aqueous conditions⁶⁴⁻⁶⁶ only permit ΔpK_a from aqueous
266 species to be used semi-quantitatively to determine the extent of proton transfer in PILs.⁶⁷

267 Complete proton transfer in PILs has been proposed to require $\Delta pK_a > 10$.⁵⁰ Because our
268 herbicide-amine salts have known ΔpK_a values ranging from 7.7-8.8 (**SI Table S2**), proton
269 transfer between the herbicide and amine is likely incomplete, resulting in the presence of
270 neutral species with a vapor pressure closer to that of their pure phase.^{50,61,62} Volatilization of
271 amines may then occur due to their high vapor pressures (**SI Table S1**). Although some PILs
272 have been measured in the gas phase as ionic pairs or aggregates^{68,69} (particularly for
273 combinations of strong acids and bases with $\Delta pK_a \geq 17.6$),⁶⁸ we believe this is unlikely to
274 dominate in our herbicide-amine salts due to the relatively low ΔpK_a values and our
275 observation that amine loss often exceeds herbicide loss (**Figure 1-3**).

276 Upon formation of other PILs, the more volatile component is observed to volatilize
277 alongside the solvent,^{58,70} similar to what we observed in our results with DMA and IPA
278 (**Figure 1A,B**). We hypothesize that DMA loss as the aqueous solution dried (**Figure 1A**) may
279 be attributed to a fraction of DMA remaining unprotonated that volatilized due to DMA's high
280 vapor pressure (**SI Table S1**). After the neutral DMA had volatilized (after 16 h), we
281 hypothesize that the remaining DMA was ionic, which prevented further significant
282 volatilization (**Figure 1A**). We expect that IPA losses during the drying period may result from
283 a similar process (**Figure 1B**).

284 At higher temperatures, proton transfer in PILs shifts towards neutral molecules^{50,51} that
285 also undergo increased volatilization. At higher temperatures, all four amines volatilize from
286 dicamba-amine salt residues (**Figure 2**), likely due to the combined temperature-dependent
287 processes of proton transfer and volatilization. At longer times at these elevated temperatures,
288 amine volatilization slows in some cases (e.g., **Figure 3A**), which we hypothesize may occur
289 when volatile neutral amines are depleted. Similarly, reduced abundance of neutral amines may
290 decrease amine volatilization when the residues are initially prepared at lower amine/dicamba
291 ratios (**Figure 3E**).

292 For herbicide-amine residues with higher melting points, a solid (cocrystal/salt) may
293 serve as a better model than a PIL. Similar to PILs, ΔpK_a values of a salt/cocrystal with a
294 defined crystal structure has been correlated with extent of proton transfer.⁷¹ Unlike PILs, the
295 minimum ΔpK_a for complete proton transfer to generate an ionic salt is much lower
296 ($\Delta pK_a > 4$),⁶³ indicating that the dried residues prepared in our study, if solid, may behave as
297 ionic salts rather than cocrystals (**SI Table S2**). Higher temperatures may promote
298 volatilization from salts/cocrystals by multiple factors, including promoting volatilization of
299 molecules or melting the salt/cocrystal to form a PIL if the melting temperature is exceeded.
300 For organic salts, increased temperature also has been found to shift the proton closer to the
301 acidic molecule⁵²⁻⁵⁴ and, in some cases, increase the length of the bond between the acid and
302 base^{52,72,73} which both may weaken interactions that may lead to increased volatilization
303 observed at higher temperatures (**Figure 2**).

304 While herbicide-amine salt formulations are typically formulated as equimolar
305 solutions, interactions may also involve multiple acidic or basic molecules. For example, some
306 carboxylic acids form hydrogen-bonded dimeric or oligomeric combinations with other
307 carboxylic acids when mixed with amines or other nitrogen containing molecules (i.e., $HA_x +$
308 $B \leftrightarrow H_{x-1}A_x^- + HB^+$),^{74,75} which may contribute to lower herbicide loss relative to amines even
309 at elevated temperatures (**Figure 1,2**). In addition, PILs of dicamba-BAPMA prepared at 2/1
310 and 3/1 molar ratios of dicamba/BAPMA demonstrated that individual BAPMA molecules
311 were capable of deprotonating multiple dicamba molecules.⁵⁷ This unique ability may explain
312 why BAPMA loss at higher temperatures plateaued when the remaining BAPMA reached a
313 $\sim 2/1$ dicamba/BAPMA molar ratio (**Figure 2D**).

314 *Estimate of Amine Application as Herbicide-Amine Salt Formulations in the U.S.*

315 To determine the magnitude of herbicide-amine salt applications on four major crops
316 (i.e., soybean, corn, cotton, wheat) that serve as a potential source of amine pollutants into the

317 atmosphere, we integrated Region State survey data from 2017 and 2018 from the U.S.
318 Department of Agriculture on type of herbicide formulation used⁴ with U.S. herbicide use
319 estimates in 2017³ (**SI Section S10**). From overall application rate of amines, we provide an
320 estimated upper limit of atmospheric input of amines from this pathway, which may motivate
321 subsequent measurements of amine fluxes in the field.

322 In the U.S., amine salt formulations comprise slightly more than half of combined
323 glyphosate, 2,4-D, and dicamba applications by mass (**Figure 4A**). Approximately half of
324 glyphosate is applied with an amine, typically IPA and – to a much lesser extent – DMA (49%
325 and 3% of total applications, respectively). In contrast, almost 90% of dicamba is applied as
326 an amine salt, which is distributed among DMA, DGA, and BAPMA (24%, 45%, and 20%
327 respectively) likely because postemergent application on GM dicamba-tolerant crops require
328 DGA and BAPMA salt formulations specifically.² Amine salt formulations for 2,4-D are
329 applied less extensively (44%) due to the prevalence of 2,4-D-ester formulations.⁷⁶

330 Variations in the inclusion of amines alongside specific herbicides affect the application
331 rates of amines on different crops, which may have important regional impacts on amine input
332 into the environment. Although total herbicide applications on soybeans and corn exceed
333 application on cotton by ~6- and 4-fold respectively (**Figure 4B**), the potential amine input (as
334 nitrogen, N) applied to those crops only exceed those from cotton by 4- and 3-fold (**Figure**
335 **4C**). This difference results largely from the fact that approximately 74% of herbicide
336 applications to cotton contained an amine (typically amine formulations of dicamba and
337 glyphosate), whereas only 48-58% of herbicide applications on the other major crops included
338 an amine counterion (**Figure 4B**).

339 Overall, the use of amines in herbicide formulations in the U.S. is estimated to input
340 about 4.0 Gg N into the environment (**Figure 4D**). The majority is IPA (3.2 Gg N) due to its
341 use with glyphosate, which is applied at a 6-fold higher rate than 2,4-D and dicamba combined

342 (Figure 4A). DMA is second (572 Mg N) due to its inclusion across salt formulations of all
343 three herbicides. Notably, these two amines have the highest vapor pressures (SI Table S1)
344 and demonstrated the greatest losses in our experiments at ambient temperatures, suggesting
345 their atmospheric flux may be particularly important. Because DGA and BAPMA are
346 exclusively applied with dicamba, which was used at the lowest rate in 2017, their potential
347 inputs are smaller (135 and 162 Mg N, respectively). Though DGA is used more often than
348 BAPMA, BAPMA salt formulations could potentially contribute more nitrogen to the
349 atmosphere due to the three amine groups present per molecule (Figure 4D).

350 Environmental Implications

351 Herein, we consistently measured amine molar losses that are greater than or equal to
352 the herbicide molar losses from the same salts, suggesting that herbicide-amine salt
353 applications are a source of amines to the atmosphere. The measurable losses of DMA and IPA
354 during drying at room temperature indicate that amine losses can occur from these herbicide-
355 amine salts at ambient temperatures. Because the amine losses often exceed herbicide losses,
356 we expect that amines are likely to be volatilizing from applications of herbicide-amine salts
357 even when off-target movement of the herbicide is not observed. Though our study is the first
358 to raise amine volatilization as a possible factor contributing to subsequent herbicide
359 volatilization, it is also apparent that extensive loss of some amines (i.e., BAPMA, Figure 2D)
360 can occur with little impact on dicamba loss, possibly because the amine molecules remaining
361 interact with multiple dicamba molecules to suppress volatilization.²⁴

362 We proposed that amine volatilization from herbicide-amine salts was enabled by
363 incomplete proton transfer between the herbicide and the amine, resulting in a fraction of the
364 molecules present as the more volatile neutral species. Recently, some permanently charged
365 organic cations have been included in commercial herbicide formulations (i.e., 2,4-D-
366 choline)⁷⁷ and researched for further use alongside 2,4-D and dicamba.^{57,78,79} These

367 permanently charged cations may have reduced volatilization compared to the basic amines
368 considered in this study.⁶² Further characterization of herbicide-amine salts (i.e., extent of
369 proton transfer, intermolecular interactions) and of vapor composition (i.e., neutral molecules,
370 aggregates, ion pairs) from herbicide-amine salts will help improve the understanding of
371 volatilization from these multicomponent systems.

372 Though this study provides the first evidence that herbicide-amine salts may be an
373 important source of atmospheric amines, the magnitude of this source would be better
374 constrained by further investigations, particularly involving field measurements. Laboratory
375 measurements from representative soil and leaf surfaces may also help to constrain the
376 magnitude of amine volatilization relative to other co-occurring processes (e.g., biological
377 uptake and transformation), as well as identify key environmental parameters. Additional
378 complexities in chemical compositions of the salts may also influence amine volatilization. For
379 example, herbicide formulations can be applied in combination, which has been shown to alter
380 herbicide volatilization^{20,24,26} and may also impact amine volatilization.

381 We found that an estimated 4.0 Gg N of amines were applied as glyphosate, dicamba,
382 and 2,4-D salt formulations during 2017 in the U.S. alone. While this number is relatively small
383 compared to the estimated 285 Gg N global flux of methylamines,²⁹ regional effects may be
384 significant. For example, herbicide-amine salt applications may provide an overlooked source
385 for atmospheric amines in rural environments, where amine-assisted particle nucleation (i.e.,
386 new particle formation) is likely to occur at low concentrations of pre-existing particles.²⁹
387 Amine volatilization from herbicide-amine salt formulations may also help rectify differences
388 in predictive models that estimate lower concentrations of atmospheric amines than what has
389 been measured particularly in rural environments.⁸⁰

390 Furthermore, our estimate only considers U.S. herbicide applications, which accounts
391 for ~12% of the herbicide use worldwide.¹ Since global use of glyphosate and 2,4-D exceeds

392 U.S. use by more than 5- and 7-fold respectively, amine formulations of these herbicides in
393 particular may be prevalent worldwide. Though use rates are unavailable, both glyphosate and
394 2,4-D-amine salt formulations are approved for use in countries such as China and Brazil⁸¹⁻⁸⁴
395 that rank with the U.S. as the top herbicide applicators globally.¹ Accounting for formulation
396 type in addition to total use¹ would help determine the global contribution of herbicide-amine
397 salt formulations to amine pollution in the atmosphere.

398 **Acknowledgements**

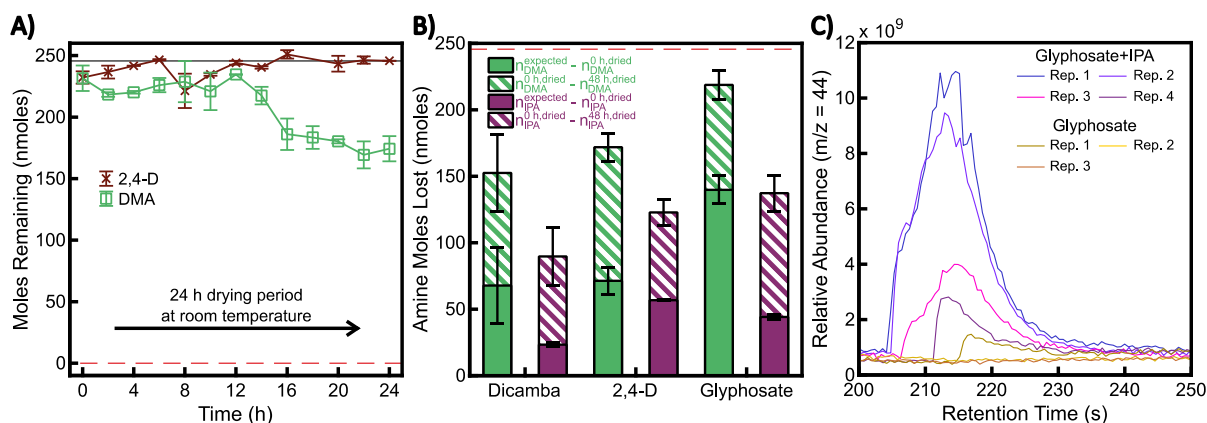
399 This work is supported by N.S.F. CAREER Award 2046602 (SMS, KMP), ACS –
400 Petroleum Research Fund 60057-DNI4 (AC, KMP), N.S.F. Graduate Research Fellowship
401 under DGE-2139839 and DGE-1745038 (AJD), and N.S.F. Award 1554061 (BJW). We would
402 like to thank Dr. Christine Wieben for providing additional information on the herbicide use
403 estimates.

404 **Supporting Information Description**

405 Chemical parameters from literature; chemicals, suppliers, and glassware cleaning; herbicide
406 and amine extraction recoveries; improving FMOC-glyphosate HPLC peak shape; amine
407 derivatization procedure; improving FMOC-BAPMA HPLC peak shape; HPLC methods; gas
408 phase measurements; measuring 2,4-D and DMA during drying; additional description of gas
409 phase measurements; calculations used to estimate amine applications.

410

411 **Figures**



412

413 **Figure 1.** Measurements of amine losses from aqueous solution and residue phases. **A)** DMA

414 and 2,4-D moles remaining during the 24 h drying period at room temperature. Solid black line

415 at 246 nmoles (123 μ M) is the expected initial aqueous amount of 2,4-D and DMA. Water

416 remaining in samples was measured and included in calculations (**SI Section S8**). **B)** DMA and

417 IPA losses during the 24 h drying period at room temperature ($n_x^{expected} - n_x^{0 h,dried}$, solid

418 bars) and the 48 h at 40°C ($n_x^{0 h,dried} - n_x^{48 h,dried}$, striped bars) from dicamba, 2,4-D, and

419 glyphosate-amine salt residues. The dashed red line indicates the expected initial moles of

420 amine and herbicide in aqueous solution (246 nmoles, 123 μ M). Herbicide molar losses from

421 the same salts are available in **SI Figure S7**. **C)** IPA peaks from chromatograms obtained using

422 TD GC-MS measurements above the headspace of vials containing equimolar glyphosate and

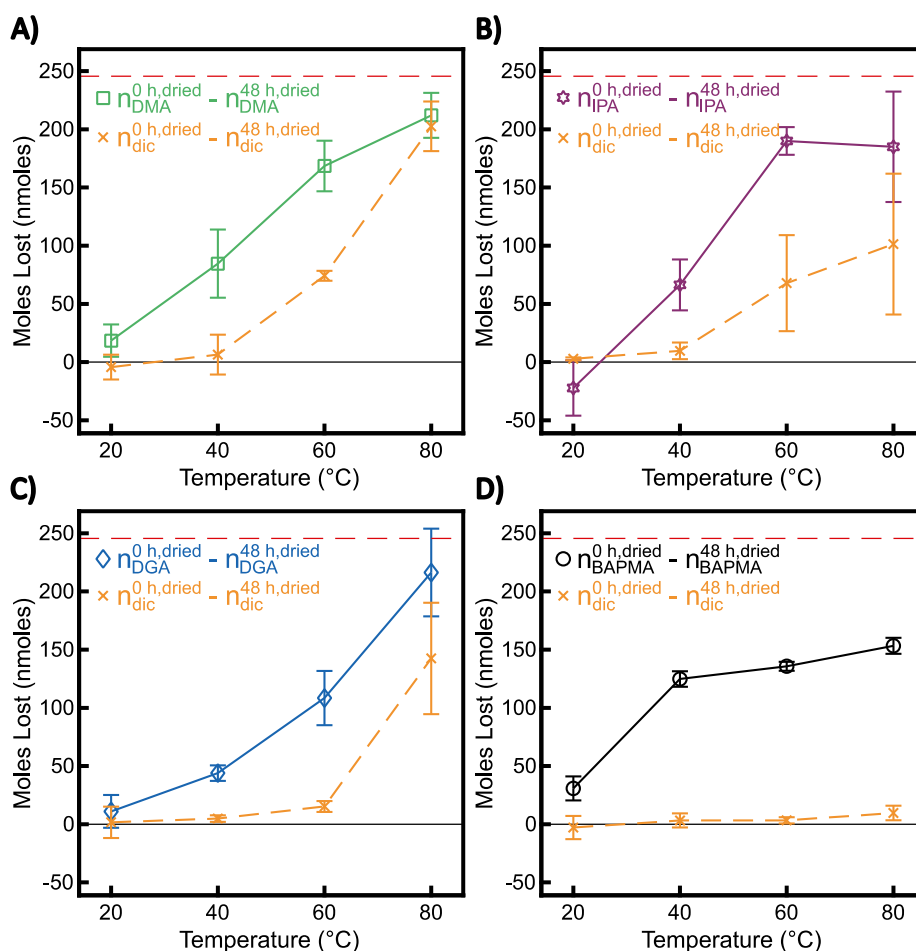
423 IPA or only glyphosate in 13.2 mM aqueous solutions. Peaks shown are the largest peaks for

424 each set of vials (6 vials for each glyphosate+IPA Rep. 1-4 and 5 vials for each glyphosate

425 Rep. 1-3) from which one vial was sampled for a 5 min duration every 20 min after sample

426 preparation. Peak areas for the other vials in each set are presented in **SI Section S9**.

427



428

429 **Figure 2.** Dicamba and amine losses from residues after 48 h. The difference between the

430 measured moles of amine and dicamba at 0 h and 48 h ($n_x^{0 \text{ h, dried}} - n_x^{48 \text{ h, dried}}$) for dicamba

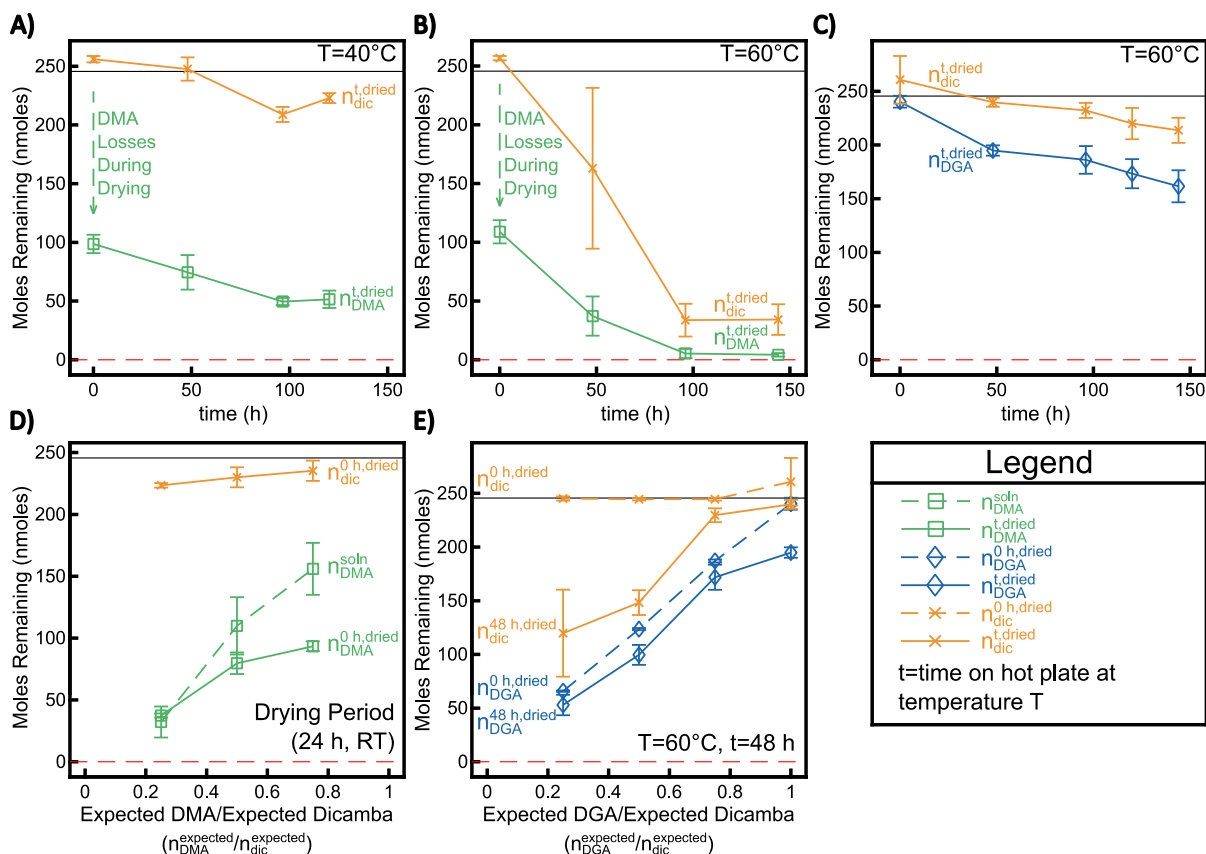
431 salt residues prepared with **A)** DMA, **B)** IPA, **C)** DGA, and **D)** BAPMA. Residues were dried

432 from 2 mL of water at room temperature for 24 h and then left on a hot plate at the specified

433 temperature for 48 h. The dashed red line indicates the expected initial moles of amines and

434 dicamba in 2 mL aqueous solution (246 nmol, 123 μM).

435



436

437 **Figure 3.** Measurements of dicamba and amine losses at longer temperatures and reduced

438 initial amine concentration in solution. DMA and dicamba moles remaining (n_x^t) **A)** at 40°C

439 and **B)** at 60°C. **C)** DGA and dicamba moles remaining (n_x^t) at 60°C. **D)** Measured moles of

440 DMA initially in solution (n_{DMA}^{soln}) and measured moles of dicamba and DMA after the 24 h

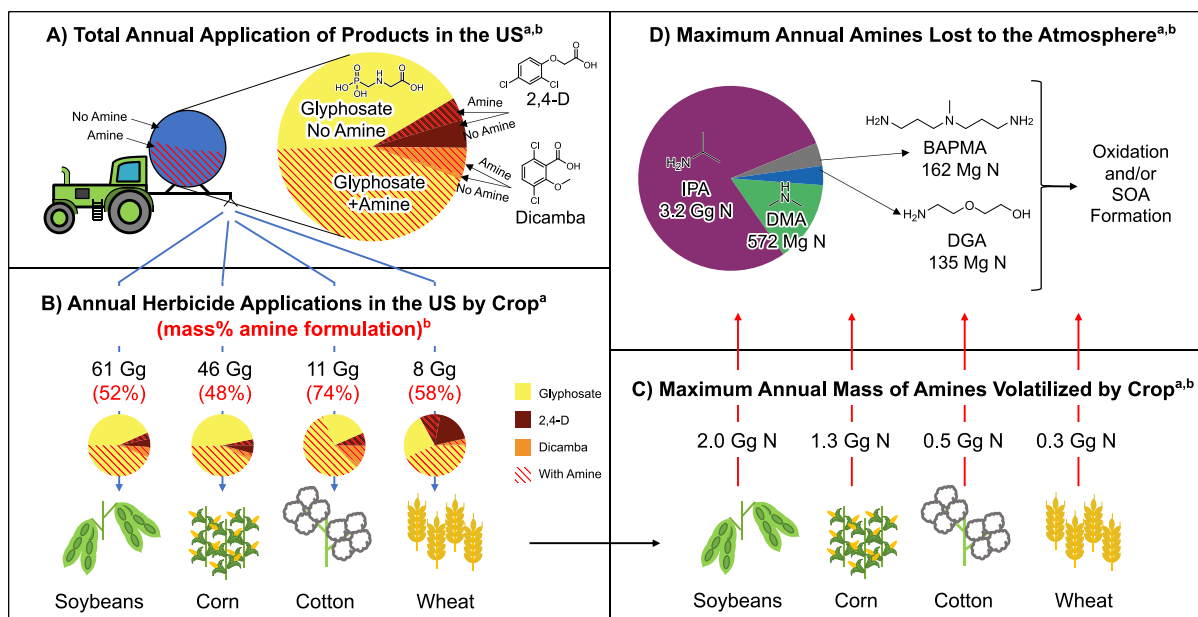
441 drying period at room temperature ($n_x^{0,h,dried}$) with reduced initial ratio of DMA to dicamba

442 ($n_{DMA}^{expected}/n_{dic}^{expected}$). **E)** Measured moles of dicamba and DGA in the dried residue before

443 ($n_x^{0,h,dried}$) and after ($n_x^{48,h,dried}$) 48 h at 60°C with reduced initial ratio of DGA to dicamba

444 ($n_{DGA}^{expected}/n_{dic}^{expected}$). All residues were dried from 2 mL of equimolar dicamba-amine

445 solutions with an expected initial concentration of 246 nmoles unless otherwise noted.



446

447 **Figure 4.** Estimations of annual amine applications and losses from herbicide-amine salt
 448 applications in the U.S. **A)** Pie chart on the back of the tractor gives total fraction of glyphosate,
 449 2,4-D, and dicamba applied to soybean, corn, cotton, and wheat with and without an amine
 450 counterion, with values broken down by herbicide in the pie chart directly to the right. **B)** Mass
 451 of herbicide applications by crop (black text), mass percent of herbicide applications that
 452 contain an amine (red text), further broken down by herbicide (pie chart). **C)** Maximum mass
 453 of amine as nitrogen (Gg N) that could be lost from each crop. **D)** Pie chart giving maximum
 454 amine losses to the atmosphere broken down by amine. Detailed description of calculations
 455 and assumptions can be found in **SI Section S10**.

456 ^aEstimated using 2017 data from Ref. 3.

457 ^bEstimated using 2017 and 2018 (when 2017 was unavailable) data from Ref. 4.

458

459 **References**

460 (1) Food and Agriculture Organization of the United Nations. *FAOSTAT Pesticide Use*.
 461 <https://www.fao.org/faostat/en/#data/RP/visualize> (accessed 2021-11-16).

462 (2) Sharkey, S. M.; Williams, B. J.; Parker, K. M. Herbicide Drift from Genetically Engineered
 463 Herbicide-Tolerant Crops. *Environ. Sci. Technol.* **2021**, *55* (23), 15559–15568.
 464 <https://doi.org/10.1021/acs.est.1c01906>.

465 (3) Wieben, C. M. Estimated Annual Agricultural Pesticide Use by Major Crop or Crop Group for
 466 States of the Conterminous United States, 1992-2017 (Ver. 2.0, May 2020), 2020.
 467 <https://doi.org/10.5066/P9HHG3CT>.

468 (4) USDA National Agricultural Statistics Service. *NASS - Quick Stats*.
 469 <https://data.nal.usda.gov/dataset/nass-quick-stats> (accessed 2020-05-14).

470 (5) Franz, J. E. N-Phosphonomethyl-Glycine Phytotoxicant Compositions US Patent No 3,799,758.
 471 3,799,758, March 26, 1974.

472 (6) Jones, F. D. Methods and Compositions for Killing Weeds US Patent No. 2,390,941. 2390941,
 473 December 11, 1945.

474 (7) Marth, P. C.; Mitchell, J. W. Comparative Volatility of Various Forms of 2,4-D. *Bot. Gaz.* **1949**,
 475 *110* (4), 632–636.

476 (8) Baskin, A. D.; Walker, E. A. The Responses of Tomato Plants to Vapors of 2,4-D and/or 2,4,5-T
 477 Formulations at Normal and Higher Temperatures. *Weeds* **1953**, *2* (4), 280–287.
 478 <https://doi.org/10.2307/4040105>.

479 (9) Behrens, R.; Lueschen, W. E. Dicamba Volatility. *Weed Sci.* **1979**, *27* (5), 486–493.
 480 <https://doi.org/10.1017/S0043174500044453>.

481 (10) Behrens, M. R.; Mutlu, N.; Chakraborty, S.; Dumitru, R.; Jiang, W. Z.; LaVallee, B. J.; Herman, P.
 482 L.; Clemente, T. E.; Weeks, D. P. Dicamba Resistance: Enlarging and Preserving Biotechnology-
 483 Based Weed Management Strategies. *Science* **2007**, *316* (5828), 1185–1188.
 484 <https://doi.org/10.1126/science.1141596>.

485 (11) Wright, T. R.; Shan, G.; Walsh, T. A.; Lira, J. M.; Cui, C.; Song, P.; Zhuang, M.; Arnold, N. L.; Lin,
 486 G.; Yau, K.; Russell, S. M.; Cicchillo, R. M.; Peterson, M. A.; Simpson, D. M.; Zhou, N.;
 487 Ponsamuel, J.; Zhang, Z. Robust Crop Resistance to Broadleaf and Grass Herbicides Provided
 488 by Aryloxyalkanoate Dioxygenase Transgenes. *Proc. Natl. Acad. Sci.* **2010**, *107* (47), 20240–
 489 20245. <https://doi.org/10.1073/pnas.1013154107>.

490 (12) Culpepper, A. S.; Sosnoskie, L. M.; Shugart, J.; Leifheit, N.; Curry, M.; Gray, T. Effects of Low-
 491 Dose Applications of 2,4-D and Dicamba on Watermelon. *Weed Technol.* **2018**, *32* (3), 267–
 492 272. <https://doi.org/10.1017/wet.2018.4>.

493 (13) Hand, L. C.; Vance, J. C.; Randell, T. M.; Shugart, J.; Gray, T.; Luo, X.; Culpepper, A. S. Effects of
 494 Low-Dose Applications of 2,4-D and Dicamba on Cucumber and Cantaloupe. *Weed Technol.*
 495 **2021**, *35* (3), 357–362. <https://doi.org/10.1017/wet.2020.129>.

496 (14) Jeffrey Brainard. News at a Glance: Bayer Funds Glyphosate Review. *Science* **2020**, *369* (6499),
 497 12–13. <https://doi.org/10.1126/science.369.6499.12>.

498 (15) Jeffrey Brainard. News at a Glance: Bayer, BASF Lose Herbicide Case. *Science* **2020**, *367*
 499 (6481), 960–961. <https://doi.org/10.1126/science.367.6481.960>.

500 (16) Iriart, V.; Baucom, R. S.; Ashman, T. Herbicides as Anthropogenic Drivers of Eco-evo
 501 Feedbacks in Plant Communities at the Agro-ecological Interface. *Mol. Ecol.* **2021**, *30* (21),
 502 5406–5421. <https://doi.org/10.1111/mec.15510>.

503 (17) Vieira, B. C.; Luck, J. D.; Amundsen, K. L.; Werle, R.; Gaines, T. A.; Kruger, G. R. Herbicide Drift
 504 Exposure Leads to Reduced Herbicide Sensitivity in *Amaranthus* Spp. *Sci. Rep.* **2020**, *10* (1),
 505 2146. <https://doi.org/10.1038/s41598-020-59126-9>.

506 (18) US Environmental Protection Agency. *Memorandum Supporting Decision to Approve*
 507 *Registration for the Uses of Dicamba on Dicamba Tolerant Cotton and Soybean*.

- 508 <https://www.regulations.gov/document/EPA-HQ-OPP-2020-0492-0007> (accessed 2020-11-
509 20).
- 510 (19) Mueller, T. C.; Wright, D. R.; Remund, K. M. Effect of Formulation and Application Time of Day
511 on Detecting Dicamba in the Air under Field Conditions. *Weed Sci.* **2013**, *61* (4), 586–593.
512 <https://doi.org/10.1614/WS-D-12-00178.1>.
- 513 (20) Bish, M. D.; Farrell, S. T.; Lerch, R. N.; Bradley, K. W. Dicamba Losses to Air after Applications
514 to Soybean under Stable and Nonstable Atmospheric Conditions. *J. Environ. Qual.* **2019**, *48*
515 (6), 1675–1682. <https://doi.org/10.2134/jeq2019.05.0197>.
- 516 (21) Bish, M.; Oseland, E.; Bradley, K. Off-Target Pesticide Movement: A Review of Our Current
517 Understanding of Drift Due to Inversions and Secondary Movement. *Weed Technol.* **2021**, *35*
518 (3), 345–356. <https://doi.org/10.1017/wet.2020.138>.
- 519 (22) Egan, J. F.; Mortensen, D. A. Quantifying Vapor Drift of Dicamba Herbicides Applied to
520 Soybean. *Environ. Toxicol. Chem.* **2012**, *31* (5), 1023–1031. <https://doi.org/10.1002/etc.1778>.
- 521 (23) Ouse, D. G.; Gifford, J. M.; Schleier, J.; Simpson, D. D.; Tank, H. H.; Jennings, C. J.; Annangudi,
522 S. P.; Valverde-Garcia, P.; Masters, R. A. A New Approach to Quantify Herbicide Volatility.
523 *Weed Technol.* **2018**, *32* (6), 691–697. <https://doi.org/10.1017/wet.2018.75>.
- 524 (24) Sharkey, S. M.; Stein, A.; Parker, K. M. Hydrogen Bonding Site Number Predicts Dicamba
525 Volatilization from Amine Salts. *Environ. Sci. Technol.* **2020**, *54* (21), 13630–13637.
526 <https://doi.org/10.1021/acs.est.0c03303>.
- 527 (25) Jones, G. T.; Norsworthy, J. K.; Barber, T.; Gbur, E.; Kruger, G. R. Off-Target Movement of DGA
528 and BAPMA Dicamba to Sensitive Soybean. *Weed Technol.* **2019**, *33* (1), 51–65.
529 <https://doi.org/10.1017/wet.2018.121>.
- 530 (26) Mueller, T. C.; Steckel, L. E. Dicamba Volatility in Humidomes as Affected by Temperature and
531 Herbicide Treatment. *Weed Technol.* **2019**, *33* (04), 541–546.
532 <https://doi.org/10.1017/wet.2019.36>.
- 533 (27) Oseland, E.; Bish, M.; Steckel, L.; Bradley, K. Identification of Environmental Factors That
534 Influence the Likelihood of Off-target Movement of Dicamba. *Pest Manag. Sci.* **2020**, *76* (9),
535 3282–3291. <https://doi.org/10.1002/ps.5887>.
- 536 (28) Sosnoskie, L. M.; Culpepper, A. S.; Braxton, L. B.; Richburg, J. S. Evaluating the Volatility of
537 Three Formulations of 2,4-D When Applied in the Field. *Weed Technol.* **2015**, *29* (2), 177–184.
538 <https://doi.org/10.1614/WT-D-14-00128.1>.
- 539 (29) Ge, X.; Wexler, A. S.; Clegg, S. L. Atmospheric Amines – Part I. A Review. *Atmos. Environ.* **2011**,
540 *45* (3), 524–546. <https://doi.org/10.1016/j.atmosenv.2010.10.012>.
- 541 (30) Pitts, J. N.; Grosjean, D.; Van Cauwenberghe, K.; Schmid, J. P.; Fitz, D. R. Photooxidation of
542 Aliphatic Amines under Simulated Atmospheric Conditions: Formation of Nitrosamines,
543 Nitramines, Amides, and Photochemical Oxidant. *Environ. Sci. Technol.* **1978**, *12* (8), 946–953.
544 <https://doi.org/10.1021/es60144a009>.
- 545 (31) Grosjean, D. Atmospheric Chemistry of Toxic Contaminants. 6. Nitrosamines: Dialkyl
546 Nitrosamines and Nitrosomorpholine. *J. Air Waste Manag. Assoc.* **1991**, *41* (3), 306–311.
547 <https://doi.org/10.1080/10473289.1991.10466847>.
- 548 (32) Tuazon, E. C.; Atkinson, R.; Aschmann, S. M.; Arey, J. Kinetics and Products of the Gas-Phase
549 Reactions of O₃ with Amines and Related Compounds. *Res. Chem. Intermed.* **1994**, *20* (3–5),
550 303–320. <https://doi.org/10.1163/156856794X00351>.
- 551 (33) Nielsen, C. J.; D’Anna, B.; Karl, M.; Aursnes, M.; Boreave, A.; Bossi, R.; Bunkan, A. J. C.; Glasius,
552 M.; Hallquist, M.; Hansen, A. M. K.; Kristensen, K.; Mikoviny, T.; Maguta, M. M.; Müller, M.;
553 Nguyen, Q.; Westerlund, J.; Salo, K.; Skov, H.; Stenstrøm, Y.; Wisthaler, A. Atmospheric
554 Degradation of Amines (ADA). Summary Report: Photo-Oxidation of Methylamine,
555 Dimethylamine and Trimethylamine. CLIMIT Project No. 201604. *NILU* **2011**.
- 556 (34) Nielsen, C. J.; D’Anna, B.; Bossi, R.; Bunkan, A. J. C.; Dithmer, L.; Glasius, M.; Hallquist, M.;
557 Hansen, A. M. K.; Lutz, A.; Salo, K.; Maguta, M. M.; Nguyen, Q.; Mikoviny, T.; Müller, M.; Skov,
558 H.; Sarrasin, E.; Stenstrøm, Y.; Tang, Y.; Westerlund, J.; Wisthaler, A. Atmospheric Degradation

- 559 of Amines (ADA). Summary Report from Atmospheric Chemistry Studies of Amines,
560 Nitrosamines, Nitramines and Amines. CLIMIT Project No. 208122. *NILU* **2012**.
- 561 (35) Lee, D.; Wexler, A. S. Atmospheric Amines – Part III: Photochemistry and Toxicity. *Atmos.*
562 *Environ.* **2013**, *71*, 95–103. <https://doi.org/10.1016/j.atmosenv.2013.01.058>.
- 563 (36) Murphy, S. M.; Sorooshian, A.; Kroll, J. H.; Ng, N. L.; Chhabra, P.; Tong, C.; Surratt, J. D.;
564 Knipping, E.; Flagan, R. C.; Seinfeld, J. H. Secondary Aerosol Formation from Atmospheric
565 Reactions of Aliphatic Amines. *Atmospheric Chem. Phys.* **2007**, *7* (9), 2313–2337.
566 <https://doi.org/10.5194/acp-7-2313-2007>.
- 567 (37) Tang, X.; Price, D.; Praske, E.; Lee, S. A.; Shattuck, M. A.; Purvis-Roberts, K.; Silva, P. J.; Asa-
568 Awuku, A.; Cocker, D. R. NO₃ Radical, OH Radical and O₃-Initiated Secondary Aerosol
569 Formation from Aliphatic Amines. *Atmos. Environ.* **2013**, *72*, 105–112.
570 <https://doi.org/10.1016/j.atmosenv.2013.02.024>.
- 571 (38) Yao, L.; Garmash, O.; Bianchi, F.; Zheng, J.; Yan, C.; Kontkanen, J.; Junninen, H.; Mazon, S. B.;
572 Ehn, M.; Paasonen, P.; Sipilä, M.; Wang, M.; Wang, X.; Xiao, S.; Chen, H.; Lu, Y.; Zhang, B.;
573 Wang, D.; Fu, Q.; Geng, F.; Li, L.; Wang, H.; Qiao, L.; Yang, X.; Chen, J.; Kerminen, V.-M.;
574 Petäjä, T.; Worsnop, D. R.; Kulmala, M.; Wang, L. Atmospheric New Particle Formation from
575 Sulfuric Acid and Amines in a Chinese Megacity. *Science* **2018**, *361* (6399), 278–281.
576 <https://doi.org/10.1126/science.aao4839>.
- 577 (39) Haywood, J.; Boucher, O. Estimates of the Direct and Indirect Radiative Forcing Due to
578 Tropospheric Aerosols: A Review. *Rev. Geophys.* **2000**, *38* (4), 513–543.
579 <https://doi.org/10.1029/1999RG000078>.
- 580 (40) Lohmann, U.; Feichter, J. Global Indirect Aerosol Effects: A Review. *Atmospheric Chem. Phys.*
581 **2005**, *5* (3), 715–737. <https://doi.org/10.5194/acp-5-715-2005>.
- 582 (41) Smith, J. N.; Barsanti, K. C.; Friedli, H. R.; Ehn, M.; Kulmala, M.; Collins, D. R.; Scheckman, J. H.;
583 Williams, B. J.; McMurry, P. H. Observations of Ammonium Salts in Atmospheric Nanoparticles
584 and Possible Climatic Implications. *Proc. Natl. Acad. Sci.* **2010**, *107* (15), 6634–6639.
585 <https://doi.org/10.1073/pnas.0912127107>.
- 586 (42) Pope, C. A.; Dockery, D. W. Health Effects of Fine Particulate Air Pollution: Lines That Connect.
587 *J. Air Waste Manag. Assoc.* **2006**, *56* (6), 709–742.
588 <https://doi.org/10.1080/10473289.2006.10464485>.
- 589 (43) Nemmar, A.; Hoylaerts, M. F.; Hoet, P. H. M.; Dinsdale, D.; Smith, T.; Xu, H.; Vermeylen, J.;
590 Nemery, B. Ultrafine Particles Affect Experimental Thrombosis in an *In Vivo* Hamster Model.
591 *Am. J. Respir. Crit. Care Med.* **2002**, *166* (7), 998–1004. [https://doi.org/10.1164/rccm.200110-](https://doi.org/10.1164/rccm.200110-026OC)
592 [026OC](https://doi.org/10.1164/rccm.200110-026OC).
- 593 (44) Hamoir, J.; Nemmar, A.; Halloy, D.; Wirth, D.; Vincke, G.; Vanderplasschen, A.; Nemery, B.;
594 Gustin, P. Effect of Polystyrene Particles on Lung Microvascular Permeability in Isolated
595 Perfused Rabbit Lungs: Role of Size and Surface Properties. *Toxicol. Appl. Pharmacol.* **2003**,
596 *190* (3), 278–285. [https://doi.org/10.1016/S0041-008X\(03\)00192-3](https://doi.org/10.1016/S0041-008X(03)00192-3).
- 597 (45) *The Pesticide Manual: A World Compendium*, 11th ed.; Tomlin, C., British Crop Protection
598 Council, Eds.; British Crop Protection Council: Farnham, Surrey, UK, 1997.
- 599 (46) Rebane, R.; Herodes, K. Comparison of Three Buffer Solutions for Amino Acid Derivatization
600 and Following Analysis by Liquid Chromatography Electrospray Mass Spectrometry. *J.*
601 *Chromatogr. A* **2012**, *1245*, 134–142. <https://doi.org/10.1016/j.chroma.2012.05.039>.
- 602 (47) Linstrom, P. NIST Chemistry WebBook, NIST Standard Reference Database 69, 1997.
603 <https://doi.org/10.18434/T4D303>.
- 604 (48) Narimani, M.; da Silva, G. Thermal Decomposition Kinetics of Glyphosate (GP) and Its
605 Metabolite Aminomethylphosphonic Acid (AMPA). *Environ. Sci. Process. Impacts* **2020**, *22* (1),
606 152–160. <https://doi.org/10.1039/C9EM00422J>.
- 607 (49) Mackie, J. C.; Kennedy, E. M. Pyrolysis of Glyphosate and Its Toxic Products. *Environ. Sci.*
608 *Technol.* **2019**, *53* (23), 13742–13747. <https://doi.org/10.1021/acs.est.9b04983>.

- 609 (50) Yoshizawa, M.; Xu, W.; Angell, C. A. Ionic Liquids by Proton Transfer: Vapor Pressure,
610 Conductivity, and the Relevance of $\Delta p K_a$ from Aqueous Solutions. *J. Am. Chem. Soc.* **2003**,
611 *125* (50), 15411–15419. <https://doi.org/10.1021/ja035783d>.
- 612 (51) Chen, K.; Wang, Y.; Yao, J.; Li, H. Equilibrium in Protic Ionic Liquids: The Degree of Proton
613 Transfer and Thermodynamic Properties. *J. Phys. Chem. B* **2018**, *122* (1), 309–315.
614 <https://doi.org/10.1021/acs.jpcc.7b10671>.
- 615 (52) Steiner, T.; Majerz, I.; Wilson, C. C. First O–H–N Hydrogen Bond with a Centered Proton
616 Obtained by Thermally Induced Proton Migration. *Angew. Chem. Int. Ed.* **2001**, *40* (14), 2651–
617 2654. [https://doi.org/10.1002/1521-3773\(20010716\)40:14<2651::AID-ANIE2651>3.0.CO;2-2](https://doi.org/10.1002/1521-3773(20010716)40:14<2651::AID-ANIE2651>3.0.CO;2-2).
- 618 (53) Cowan, J. A.; Howard, J. A. K.; McIntyre, G. J.; Lo, S. M.-F.; Williams, I. D. Variable-
619 Temperature Neutron Diffraction Studies of the Short, Strong N...O Hydrogen Bonds in the
620 1:2 Co-Crystal of Benzene-1,2,4,5-Tetracarboxylic Acid and 4,4'-Bipyridyl. *Acta Crystallogr. B*
621 **2003**, *59* (6), 794–801. <https://doi.org/10.1107/S0108768103024984>.
- 622 (54) Parkin, A.; Harte, S. M.; Goeta, A. E.; Wilson, C. C. Imaging Proton Migration from X-Rays and
623 Neutrons. *New J. Chem.* **2004**, *28* (6), 718. <https://doi.org/10.1039/b315515c>.
- 624 (55) Verevkin, S. P.; Tong, B.; Welz-Biermann, U.; Chernyak, Y. Vapor Pressures and Enthalpies of
625 Vaporization of a Series of Low-Volatile Alkanolamines. *J. Chem. Eng. Data* **2011**, *56* (12),
626 4400–4406. <https://doi.org/10.1021/je2002489>.
- 627 (56) Kapteina, S.; Slowik, K.; Verevkin, S. P.; Heintz, A. Vapor Pressures and Vaporization
628 Enthalpies of a Series of Ethanolamines. *J. Chem. Eng. Data* **2005**, *50* (2), 398–402.
629 <https://doi.org/10.1021/je049761y>.
- 630 (57) Pernak, J.; Kaczmarek, D. K.; Rzemieniecki, T.; Niemczak, M.; Chrzanowski, Ł.; Praczyk, T.
631 Dicamba-Based Herbicides: Herbicidal Ionic Liquids versus Commercial Forms. *J. Agric. Food*
632 *Chem.* **2020**, *68* (16), 4588–4594. <https://doi.org/10.1021/acs.jafc.0c00632>.
- 633 (58) Burrell, G. L.; Burgar, I. M.; Separovic, F.; Dunlop, N. F. Preparation of Protic Ionic Liquids with
634 Minimal Water Content and 15N NMR Study of Proton Transfer. *Phys. Chem. Chem. Phys.*
635 **2010**, *12* (7), 1571. <https://doi.org/10.1039/b921432a>.
- 636 (59) Infantes, L.; Fábíán, L.; Motherwell, W. D. S. Organic Crystal Hydrates: What Are the
637 Important Factors for Formation. *CrystEngComm* **2007**, *9* (1), 65–71.
638 <https://doi.org/10.1039/B612529H>.
- 639 (60) Desiraju, G. R. Hydration in Organic Crystals: Prediction from Molecular Structure. *J. Chem.*
640 *Soc. Chem. Commun.* **1991**, No. 6, 426. <https://doi.org/10.1039/c39910000426>.
- 641 (61) MacFarlane, D. R.; Pringle, J. M.; Johansson, K. M.; Forsyth, S. A.; Forsyth, M. Lewis Base Ionic
642 Liquids. *Chem. Commun.* **2006**, No. 18, 1905. <https://doi.org/10.1039/b516961p>.
- 643 (62) Lopes, J. N. C.; Rebelo, L. P. N. Ionic Liquids and Reactive Azeotropes: The Continuity of the
644 Aprotic and Protic Classes. *Phys. Chem. Chem. Phys.* **2010**, *12* (8), 1948.
645 <https://doi.org/10.1039/b922524m>.
- 646 (63) Cruz-Cabeza, A. J. Acid–Base Crystalline Complexes and the PKa Rule. *CrystEngComm* **2012**, *14*
647 (20), 6362. <https://doi.org/10.1039/c2ce26055g>.
- 648 (64) Kanzaki, R.; Uchida, K.; Hara, S.; Umabayashi, Y.; Ishiguro, S.; Nomura, S. Acid–Base Property
649 of Ethylammonium Nitrate Ionic Liquid Directly Obtained Using Ion-Selective Field Effect
650 Transistor Electrode. *Chem. Lett.* **2007**, *36* (5), 684–685. <https://doi.org/10.1246/cl.2007.684>.
- 651 (65) Kanzaki, R.; Uchida, K.; Song, X.; Umabayashi, Y.; Ishiguro, S. Acidity and Basicity of Aqueous
652 Mixtures of a Protic Ionic Liquid, Ethylammonium Nitrate. *Anal. Sci.* **2008**, *24* (10), 1347–1349.
653 <https://doi.org/10.2116/analsci.24.1347>.
- 654 (66) Stoimenovski, J.; Izgorodina, E. I.; MacFarlane, D. R. Ionicity and Proton Transfer in Protic Ionic
655 Liquids. *Phys. Chem. Chem. Phys.* **2010**, *12* (35), 10341. <https://doi.org/10.1039/c0cp00239a>.
- 656 (67) Belieres, J.-P.; Angell, C. A. Protic Ionic Liquids: Preparation, Characterization, and Proton Free
657 Energy Level Representation. *J. Phys. Chem. B* **2007**, *111* (18), 4926–4937.
658 <https://doi.org/10.1021/jp067589u>.

- 659 (68) Horikawa, M.; Akai, N.; Kawai, A.; Shibuya, K. Vaporization of Protic Ionic Liquids Studied by
660 Matrix-Isolation Fourier Transform Infrared Spectroscopy. *J. Phys. Chem. A* **2014**, *118* (18),
661 3280–3287. <https://doi.org/10.1021/jp501784w>.
- 662 (69) Zhu, X.; Wang, Y.; Li, H. Do All the Protic Ionic Liquids Exist as Molecular Aggregates in the Gas
663 Phase? *Phys. Chem. Chem. Phys.* **2011**, *13* (39), 17445. <https://doi.org/10.1039/c1cp21817d>.
- 664 (70) Zhao, C.; Burrell, G.; Torriero, A. A. J.; Separovic, F.; Dunlop, N. F.; MacFarlane, D. R.; Bond, A.
665 M. Electrochemistry of Room Temperature Protic Ionic Liquids. *J. Phys. Chem. B* **2008**, *112*
666 (23), 6923–6936. <https://doi.org/10.1021/jp711804j>.
- 667 (71) Gilli, P.; Pretto, L.; Bertolasi, V.; Gilli, G. Predicting Hydrogen-Bond Strengths from Acid–Base
668 Molecular Properties. The PK_a Slide Rule: Toward the Solution of a Long-Lasting Problem. *Acc.*
669 *Chem. Res.* **2009**, *42* (1), 33–44. <https://doi.org/10.1021/ar800001k>.
- 670 (72) Bhattacharya, S.; Saraswatula, V. G.; Saha, B. K. Thermal Expansion in Alkane Diacids—
671 Another Property Showing Alternation in an Odd–Even Series. *Cryst. Growth Des.* **2013**, *13*
672 (8), 3651–3656. <https://doi.org/10.1021/cg400668w>.
- 673 (73) Das, D.; Barbour, L. J. Uniaxial Negative Thermal Expansion Induced by Moiety Twisting in an
674 Organic Crystal. *CrystEngComm* **2018**, *20* (35), 5123–5126.
675 <https://doi.org/10.1039/C8CE01169A>.
- 676 (74) Johansson, K. M.; Izgorodina, E. I.; Forsyth, M.; MacFarlane, D. R.; Seddon, K. R. Protic Ionic
677 Liquids Based on the Dimeric and Oligomeric Anions: [(AcO)XHx–1][–]. *Phys. Chem. Chem. Phys.*
678 **2008**, *10* (20), 2972. <https://doi.org/10.1039/b801405a>.
- 679 (75) Kohler, F.; Atrops, H.; Kalali, H.; Liebermann, E.; Wilhelm, E.; Ratkovics, F.; Salamon, T.
680 Molecular Interactions in Mixtures of Carboxylic Acids with Amines. 1. Melting Curves and
681 Viscosities. *J. Phys. Chem.* **1981**, *85* (17), 2520–2524. <https://doi.org/10.1021/j150617a021>.
- 682 (76) Peterson, M. A.; McMaster, S. A.; Riechers, D. E.; Skelton, J.; Stahlman, P. W. 2,4-D Past,
683 Present, and Future: A Review. *Weed Technol.* **2016**, *30* (2), 303–345.
684 <https://doi.org/10.1614/WT-D-15-00131.1>.
- 685 (77) US Environmental Protection Agency. *Final Registration of Enlist Duo Herbicide*.
686 [https://www.epa.gov/sites/production/files/2014-10/documents/final_registration_-](https://www.epa.gov/sites/production/files/2014-10/documents/final_registration_-_enlist_duo.pdf)
687 [_enlist_duo.pdf](https://www.epa.gov/sites/production/files/2014-10/documents/final_registration_-_enlist_duo.pdf) (accessed 2020-12-16).
- 688 (78) Choudhary, H.; Pernak, J.; Shamshina, J. L.; Niemczak, M.; Giszter, R.; Chrzanowski, Ł.; Praczyk,
689 T.; Marcinkowska, K.; Cojocar, O. A.; Rogers, R. D. Two Herbicides in a Single Compound:
690 Double Salt Herbicidal Ionic Liquids Exemplified with Glyphosate, Dicamba, and MCPA. *ACS*
691 *Sustain. Chem. Eng.* **2017**, *5* (7), 6261–6273.
692 <https://doi.org/10.1021/acssuschemeng.7b01224>.
- 693 (79) Niu, J.; Zhang, Z.; Tang, J.; Tang, G.; Yang, J.; Wang, W.; Huo, H.; Jiang, N.; Li, J.; Cao, Y.
694 Dicationic Ionic Liquids of Herbicide 2,4-Dichlorophenoxyacetic Acid with Reduced Negative
695 Effects on Environment. *J. Agric. Food Chem.* **2018**, *66* (40), 10362–10368.
696 <https://doi.org/10.1021/acs.jafc.8b02584>.
- 697 (80) Yu, F.; Luo, G. Modeling of Gaseous Methylamines in the Global Atmosphere: Impacts of
698 Oxidation and Aerosol Uptake. *Atmospheric Chem. Phys.* **2014**, *14* (22), 12455–12464.
699 <https://doi.org/10.5194/acp-14-12455-2014>.
- 700 (81) Institute Control of Agrochemicals, Ministry of Agriculture China. *China Pesticide Information*
701 *Network*. <http://www.chinapesticide.org.cn/sjzx4ywb/index.jhtml> (accessed 2022-03-01).
- 702 (82) Brazil Ministry of Agriculture, Livestock and Food supply. *2,4-D-Dimethylammonium*.
703 http://agrofit.agricultura.gov.br/agrofit_cons/principal_agrofit_cons (accessed 2022-03-01).
- 704 (83) Brazil Ministry of Agriculture, Livestock and Food supply. *Glyphosate Dimethylammonium*
705 *Salt*.
706 [http://agrofit.agricultura.gov.br/agrofit_cons/lap_ing_ativo_detalhe_cons?p_id_ingrediente](http://agrofit.agricultura.gov.br/agrofit_cons/lap_ing_ativo_detalhe_cons?p_id_ingrediente_ativo=663)
707 [_ativo=663](http://agrofit.agricultura.gov.br/agrofit_cons/lap_ing_ativo_detalhe_cons?p_id_ingrediente_ativo=663) (accessed 2022-03-01).

708 (84) Brazil Ministry of Agriculture, Livestock and Food supply. *Glyphosate-Isopropylammonium*.
709 http://agrofit.agricultura.gov.br/agrofit_cons/lap_ing_ativo_detalhe_cons?p_id_ingredientes_ativo=318 (accessed 2022-03-01).
710
711